scientific reports

Check for updates

OPEN

Biofilm-based biocatalysis for β-cyclodextrin production by the surface-display of β-cyclodextrin glycosyltransferase in *Bacillus subtilis*

Dan Wang[1,2], Sinan Wang[1,2], Wenjun Sun[1,2]✉, Tianpeng Chen[1,2]✉, Caice Liang[1,2], Pengpeng Yang[1,2], Qingguo Liu[1,3], Chunguang Zhao[4] & Yong Chen[1,2]

β-cyclodextrin (β-CD) is an important cyclic oligosaccharide, which is widely applicated in foods, environmental protection, and cosmetics, primarily prepared from enzymatic synthesis in traditional industry. However, several challenges persist, including cumbersome processes and difficulties in achieving continuous fermentation and catalysis. This research introduced a biofilm-based immobilized fermentation, integrating with enzyme catalysis system of surface display in *Bacillus subtilis*. The *bslA* gene was selected to construct the surface display system due to its ability to promote biofilm formation and serve as an anchorin. Compared to free cell catalysis, the biofilm-based immobilized catalysis expanded the temperature range to 40–70 and the pH range to 5–7.5. During the continuous catalysis process, by the 13th batch, the relative activity remained around 52%, and the conversion rate exceeded 36%, similar to the single-batch free cell catalysis. These findings provide valuable insights and effective strategies for the industrial production of β-CD and other biochemicals through continuous catalysis.

Keywords *Bacillus subtilis* surface display, Biofilm, B-cyclodextrin, B-cyclodextrin glycosyltransferase

β-Cyclodextrin (β-CD) is a cyclic oligosaccharide composed of seven D-glucopyranose monomers linked by α-1,4-glycosidic bonds[1]. Due to its cylindrical structure, which was hydrophobic internally and hydrophilic externally[2], it could be used in the stabilizer, adsorbent, surfactant and other products in food, environmental protection, cosmetics and other fields[3–6]. Currently, the enzymatic synthesis for β-CD production is the main method. More precisely, the starch was utilized as the substrate and involved a unique cyclization reaction catalyzed by β-cyclodextrin glucosyltransferase (β-CGTase) to produce β-CD[7,8]. Although large-scale β-CD production had been performed for decades, the traditional production modes (planktonic or immobilized fermentation) had not made substantial progress[9–11], which was limit in the industrial production to a certain extent.

Due to advantages such as simplicity, rapidity, and environmental friendliness in enzyme purification, along with reduced costs, enzyme surface display technology has gained global attention in biocatalysis[12,13]. Furthermore, *Bacillus subtilis* (*B. subtilis*), known for its efficient protein secretion[14], established safety profile[15], and widespread application in industrial fermentation, was employed as a biosafe strain in the food and pharmaceutical sectors[16,17]. Although spore surface display was used widely in *B. subtilis*, the harvesting, purification, and separation of spores required additional costs and labor[18]. Recently, a glucose-tolerant β-glucosidase (UnBgl1A) was displayed on the surface of *B. subtilis* using CWB_b as the anchorin, that the catalytic activity was higher than the intracellular expression of enzyme[19]. Hence, we constructed surface display system with anchorin by using *B. subtilis* as chassis cell.

[1]National Engineering Research Center for Biotechnology, College of Biotechnology and Pharmaceutical Engineering, Nanjing Tech University, Nanjing, China. [2]State Key Laboratory of Materials-Oriented Chemical Engineering, College of Biotechnology and Pharmaceutical Engineering, Nanjing Tech University, Nanjing, China. [3]Nanjing Hi-Tech Biological Technology Research Institute Co. Ltd, Nanjing, China. [4]Ningxia Yipin Biotechnology Co. Ltd, Yinchuan, China. ✉email: sunwenjun@njtech.edu.cn; chentianpeng@njtech.edu.cn

Currently, one thing that cannot be ignored is that the free fermentation has brought some problems such as increased costs because of unrecyclable cells. Besides, the environmental stress and autolysis alterations during the catalytic process resulted in a decrease of the surface displayed enzyme activity. Biofilms enable cells to gather in a well-fed environment, and isolate cells from various external pressures, such as oxidative stress, osmotic pressure, heat shock and other factors that are not conducive to cell survival and proliferation[20]. Benefited by it, the biofilm-based immobilized fermentation had been proposed owing to its advantages such as protection by the biofilm matrix, enhanced metabolic activities, and reused cells compared with free cells fermentation process[21,22], which had been applied to immobilized continuous fermentation for bioethanol fermentation and other organic chemical production[23].

In *B. subtilis*, the biofilm-associated gene *bslA* encoded the surface hydrophobic protein BslA[24], which was located on the plasma membrane of the cell and extended beyond the cell wall, promoting intercellular adhesion and forming dense biofilm[25]. Besides, it was also one of the anchorins for surface display system by forming a fusion protein with the target protein on the cell surface[26]. Therefore, we chose gene *bslA* for our study.

Here, we proposed the biofilm-based continuous catalysis integrated with surface display by combining all the advantages. Firstly, we confirmed the function of *bslA* gene in the biofilm formation. Then, β-CGTase was displayed on the surface of *B. subtilis* cells by using BslA as the anchorin. Finally, we constructed the biofilm-based immobilized fermentation integrated with enzyme catalysis by using cotton fibers as carriers (Fig. 1), which the enhanced enzyme tolerance, shortened fermentation cycle and increased biocatalytic efficiency were achieved, that provided a successful case for continuous biocatalysis of biofilm-based surface display.

Materials and methods

Strains and plasmids

B. subtilis WB600 was chosen as the study organism, and it knocked out 6 extracellular proteases and effectively improved the expression of heterrologous proteins. Meanwhile, we knocked out the *amyE* gene coded the amylase of the strain WB600 in this manuscript, which still named WB600. The gene *cgt*, encoding β-cyclodextrin glycosyltransferase, was sourced from *Bacillus circulans* 251[27], codon-optimized, and stored in plasmids pUC57. The anchorin, BslA, originated from strain 168. Plasmid pBE2R was used to construct overexpressing *bslA* and surface displayed strains. It was also used to construct strain that overexpressing *cgt* gene. For the knockdown of *bslA* in strain WB600, pJOE8999 was employed (Table 1). The sequences of primers were listed in supplymentary Table S1.

Media and growth conditions

The culture of strain WB600 took place in LB medium, which consisted of yeast extract (5 g/L), peptone (10 g/L), and NaCl (10 g/L) at a temperature of 37 °C. Solid media were prepared by adding 1.6% (w/v) agar in all instances. For the fermentation medium, the components included glucose (50 g/L), corn steep powder (25 g/L), yeast extract (5 g/L), $(NH_4)_2SO_4$ (5 g/L), K_2HPO_4 (19.2 g/L), KH_2PO_4 (2.7 g/L), and $MgSO_4$ (0.5 g/L). Mutants

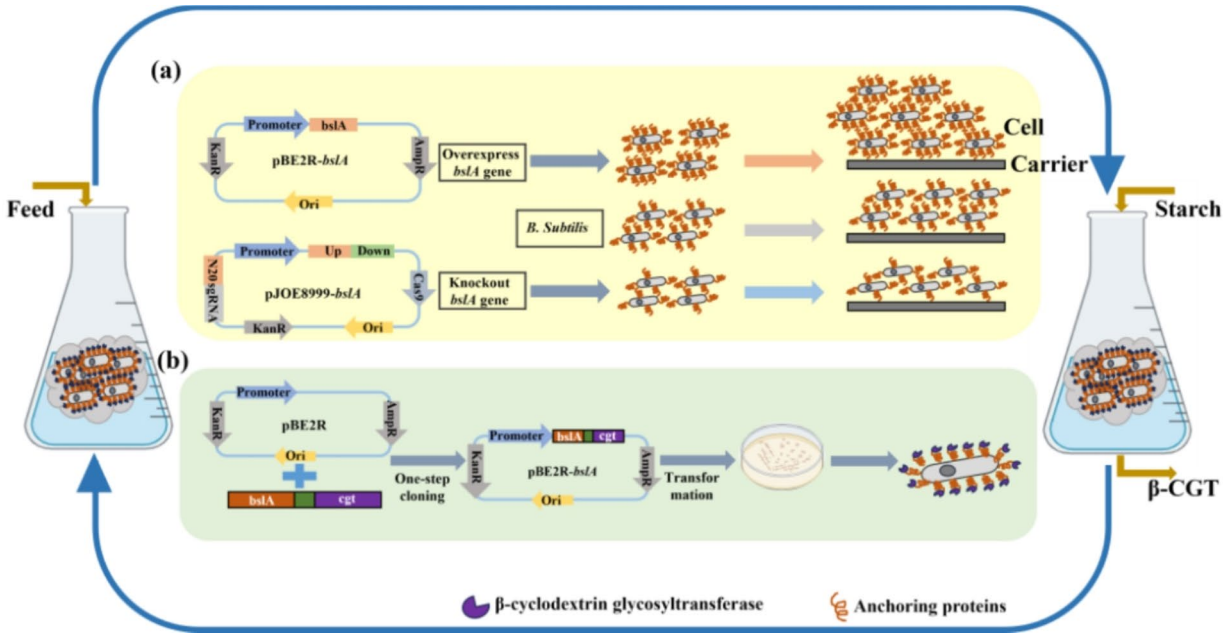

Fig. 1. Biofilm-based fermentation and biocatalysis for surface-displayed strain in dynamic growth and catalytic β-CGT production. (**a**) Effects of *bslA* gene knockout and overexpression on biofilms in *Bacillus subtilis*. (**b**) The DNA components of the surface-displayed plasmids used in this study and a schematic diagram of the *Bacillus subtilis* surface display.

Strains or plasmids	Relevant characteristics	Sources
Strains		
B. subtilis 168(168)		Stored in our lab
WB600	(*B. subtilis* 168) Δ*nprE*, Δ*aprA*, Δ*epr*, Δ*bpr*, Δ*mpr*, Δ*nprB*, Δ*amyE* Resistance to Erythromycin	Stored in our lab
+bslA	WB600 with the overexpression of *bslA*	This study
ΔbslA	WB600 with the deletion of *bslA*	This study
WB600-bslA-cgt	*cgt* comes from plasmid pUC57	This study
WB600-cgt	Free expression of β-CGTase in strain WB600	This study
Plasmids		
pBE2R	Resistance to Ampicillin	Stored in our lab
pJOE8999	Resistance to Ampicillin	Stored in our lab
pUC57	Resistance to Kanamycin	Stored in our lab

Table 1. Strains and plasmids used in this study.

were selected using 10 mg/L kanamycin (Kan) and 100 mg/L ampicillin (Amp). The strains were cultured and fermented at 37 °C with 180 rpm.

Construction of gene overexpression, knock-out, and surface-displayed strains

The hydrophobic protein BslA fragment was amplified by PCR, utilizing the strain 168 genome as a template. The primers used were shown in Supplementary Table S1. The plasmid pBE2R was linearized and fused with the *bslA* fragment to construct a recombinant plasmid. Subsequently, this plasmid was transformed into the competent cells of strain WB600, constructing a strain overexpressing *bslA*, designated as strain + bslA. The sgRNA and homologous fragment (Donor DNA) of *bslA* gene were constructed by plasmid pJOE8999, and *bslA* gene was knocked out of strain WB600 by homologous recombination, which was designated as strain ΔbslA. The expression of *cgt* gene was constructed with plasmid pBE2R and then transformed into the host to obtain strain WB600-cgt. To construct surface-displayed strain, a recombinant plasmid for surface display was firstly constructed using plasmid pBE2R. To reduce steric hindrance, a linker was used to connect the anchor protein and the target protein[28]. Here, we employed an optimized linker with the following sequence: AAAGAATCTGG CTCTGTTTCTTCTGAACAACTTGCTCAATTCCGTTCTCTTGAT. Subsequently, the recombinant plasmid was transformed into strain WB600 to obtain surface-displayed strain, designated as WB600-bslA-cgt.

Validation of the effect of hydrophobic protein BslA on biofilms

Growth curve

Bacterial biomass was determined by measuring absorbance at a wavelength of 600 nm. After overnight culturing, the strains WB600, +bslA and ΔbslA were diluted to OD_{600} = 0.1 in LB and inoculated into fresh LB with corresponding resistance. After the samples were taken within 0–24 h, the optical density of 600 nm was measured by UV spectrophotometer, and the growth curves were drawn.

Microbial adhesion to hydrocarbons (MATH)

The strains WB600, +bslA and ΔbslA were cultured at 37 °C and 180 rpm for 12 h, with the corresponding resistance added. After culture, cells were collected by centrifugation at 8000 rpm for 10 min at 4 °C to remove supernatant, and resuspended in PBS (pH 6.0). The OD_{600} of cell suspension was adjusted to 0.8-1.0, and this value was recorded as A0. Mixed 4.8 mL of cell suspension with 0.8 mL of n-hexadecane and vortexed for 90 s to ensure uniform dispersion of n-hexadecane into small droplets within the aqueous phase (the time could be extended appropriately). The water-oil mixture was allowed to stand at room temperature for 10 min to ensure complete phase separation. The aqueous phase at the bottom after separation was absorbed with a syringe, and measured its OD_{600} value, which was recorded as A1. The experiment should be completed within 1 h. Cell surface hydrophobicity was calculated as Eq. (1)[29].

$$\text{Cell surface hydrophobicity}(\%) = (1 - \text{A1}/\text{A0}) * 100 \quad (1)$$

Biofilm phenotype

The strains WB600, +bslA and ΔbslA were cultured at 37 °C and 180 rpm for 12 h. The optical density of three strains was measured with a UV spectrophotometer and they were diluted to OD_{600} = 0.1 in LB. Then 200 μL cell suspensions with different dilution ratios were transferred to a 6-well microtiter plate containing 5 mL fresh LB medium, and cultured at 30 °C for 72 h.

Biofilm formation assay

CV (crystal violet) is a basic dye commonly used to assess biofilm formation by binding and staining various substances, including negatively charged surface molecules, cells, proteins, and polysaccharides[30–33]. The strains WB600, +bslA, and ΔbslA were cultured at 37 °C and 180 rpm for 12 h. After culture, they were diluted to OD_{600} = 0.1 in LB. Then 20 μL cell suspensions were transferred to a 96-well microtiter plate containing 180 μL fresh LB medium. The microtiter plates were incubated at 30 °C for 48 h, and three parallel wells were used for

each treatment. After incubation, the wells containing biofilms were washed twice with 200 µL PBS to remove free cells. The biofilms were then stained with 200 µL of a 0.1% CV solution for 15 min at room temperature (approximately 25 °C). Following staining, the wells were repeatedly washed with PBS. Subsequently, 200 µL of 33% acetic acid was added to each well, and the plate was incubated at room temperature for 45 min with slight shaking to elute the CV. Finally, the absorbance was measured at 570 nm using a microplate reader.

Hydrolysis (starch-degrading activity)
The strains WB600 and WB600-bslA-cgt trains were cultured at 37 °C and 180 rpm for 12 h, with the corresponding resistance added. The cultures were diluted to OD_{600} = 0.1 in LB. Subsequently, 2 µL cell suspensions were inoculated into starch medium plate and incubated at 30 °C for 72 h. After the incubation, 0.02 mol/L iodine solution was added to the starch plate, and the hydrolysis circle was observed[34].

Surface-displayed β-CGTase assay

β-CGTase enzyme activity determination
Colorimetric method was used to detect the enzyme activity of β-CGTase and its standard curve drawn[35,36]. The enzyme activity of β-CGTase was determined as follows. The WB600-cgt and WB600-bslA-cgt strains were cultured at 37 °C and 180 rpm for 12 h. After culture, 1 mL cells were collected by centrifugation at 5000 rpm for 10 min to remove supernatant, and resuspended in 1 mL 25 mmol/L Na_2HPO_4-KH_2PO_4 buffer (pH 5.5). It was crude enzyme solution. 2 mL enzymatic reaction solution (a 1% starch solution dissolved in Na_2HPO4-KH_2PO4 buffer) was incubated at 50 °C for 10 min. Then, added 0.1 mL of crude enzyme solution and incubated for another 10 min. Strain WB600 was used as control. Afterward, added 0.2 mL of 0.6 mol/L HCl solution to terminate the reaction. Added 0.5 mL of 0.6 mol/L Na_2CO_3 solution to adjust the pH = 10.0. Finally, added 0.2 mL of 1.2 mmol/L phenolphthalein solution and mixed well. Allowed it to colorize at 25 °C for 15 min. Added 150 µL of sterile water to each well of a 96-well plate, followed by adding 50 µL of the chromogenic solution. Performed triplicates for each sample, and OD_{550} was detected and recorded with ELIASA. An enzyme activity unit (U) was defined as the amount of enzyme required to produce 1 µmol β-cyclodextrin within 1 min under the above assay conditions.

Detection of enzymatic activity in different parts of the bacterial suspension
The WB600-bslA-cgt and WB600-cgt strains were cultured at 37 °C and 180 rpm for 12 h. After culture, 10 mL cell suspensions were centrifuged at 5000 rpm for 10 min to obtain the supernatant, which was referred to as the fermentation supernatant. The sludge was resuspended in 5 mL of PBS buffer and sonicated for 30 min using an ultrasonic cell disruptor. Subsequently, the suspension was centrifuged at 5000 rpm for 10 min to obtain the intracellular fluid, while the sludge constituted the cell debris. The fermentation supernatant, intracellular fluid, and cell debris from WB600-bslA-cgt and WB600-cgt strains were collected separately for the determination of β-CGTase enzyme activity. The enzyme activity was determined by the same method as section "β-CGTase enzyme activity determination".

Enzymatic properties of β-CGTase
The WB600-bslA-cgt and WB600-cgt strains were used as controls. Different temperatures were set as variables during the reaction between the crude enzyme solution and the enzymatic reaction solution. The temperature settings were 30 °C, 40 °C, 50 °C, 60 °C and 70 °C respectively, and the reaction time was 10 min. The crude enzyme solution of the two strains was placed in a water bath at different temperatures to keep warm, and the temperature was set at 30 °C, 40 °C and 50 °C, respectively. After holding for 0 h, 4 h, 8 h, 12 h and 24 h, part of the crude enzyme solution was taken to react with the enzymatic reaction solution. The reaction temperature was 50 °C and the reaction time was 10 min. The sludge of the two strains was resuspended with Na_2HPO_4-KH_2PO_4 buffer at different pH to obtain crude enzyme solution at different pH. Settings of 4.0, 5.0, 6.0, 7.0 and 8.0, and the crude enzyme solution was reacted with the substrate. The crude enzyme solution of different pH was stored at 25 °C for 0 h, 4 h, 8 h, 12 h and 24 h respectively, and a part of the crude enzyme solution was taken to react with the substrate. The enzyme activity under the above four reaction conditions was determined by the same method as section "β-CGTase enzyme activity determination".

Single-batch immobilized fermentation and catalysis

Strain WB600 was cultured to obtain seed liquid. After the OD_{600} of the seed solution was diluted to about 0.1, 5 mL seed solution was inoculated into 500 mL triangular flask containing 100 mL fermentation medium and pretreated immobilized carrier and 500 mL triangular flask containing 100 mL fermentation medium at 37 °C, 180 rpm respectively. Single-batch immobilized fermentation and single-batch free cells fermentation were performed at 180 rpm for 72 h. In the single-batch catalytic process, after 72 h of culture, the fermentation medium was poured out to measure the glucose content. The medium was removed from the carrier with sterile tweezers and 100 mL of enzyme activity reaction solution was added for enzyme catalyzed reaction to determine the relative enzyme activity. In the process of single-batch free cells catalysis, 2 ml fermentation broth was used to measure glucose content and relative activity. The catalytic reaction was carried out at 37 °C and 150 rpm, and an immobilized carrier and 2 ml fermentation supernatant were taken out every 12 h for determination. Three parallel in each group. The enzyme activity was assessed using the same method as section "β-CGTase enzyme activity determination". The maximum enzyme activity of 72 h was defined as 100%. The α-CD, β-CD and γ-CD content were analyzed using HPLC. The analysis of α-CD, β-CD and γ-CD was performed on an Agilent 1260 RID-10 A instrument and an Agilent ZORBAX NH_2 analytical HPLC column at 40 °C with 65% acetonitrile mobile phase and a flow rate of 0.5 mL/min. β-cyclodextrin conversion rate was calculated as Eq. (2).

$$\beta\text{-CD conversion rate}/\% = \frac{\text{The production of } \beta\text{-CD (g)}}{\text{The quality of the initial starch (g)}} \times 100\% \quad (2)$$

Multiple batches immobilized continuous catalysis

The steps and conditions of culture and catalytic reaction of strain WB600-bslA-cgt were shown to be the same as 2.6. In the catalytic stage, a new enzymatic reaction solution was replaced 36 h after each reaction, and the catalytic reaction was ended until the relative enzyme activity dropped below 60%. Fresh medium was added to resuscitate the cells, and the catalytic process was repeated.

Scanning Electron Microscopy (SEM) of biofilm on carrier

Take the carriers after 24 h and 72 h of fermentation, the carrier after 36 h of biocatalysis, and the carrier after 24 h of recovery, respectively. The specific operation steps of carrier sample preparation were as follows: the immobilized carrier removed from the fermentation solution was cleaned three times with PBS buffer (until the buffer after cleaning was clear and transparent), and placed in a −80 °C freezer and freezing for 12 h (Labconco, Fort Scott, Kansas, USA). After freezing, the samples were quickly transferred to vacuum freeze-drying machine for drying, and observed with scanning electron microscopy.

Results and discussion

The impacts of hydrophobic protein BslA on biofilm formation in strain WB600

The growth curves of the strains WB600, ΔbslA, and +bslA were detected and variation trends were similar (Fig. 2a), which suggested that the overexpression of *bslA* gene has minimal impact on the overall growth of strain WB600. Subsequently, the influence of the BslA protein on the hydrophobicity of the strain was

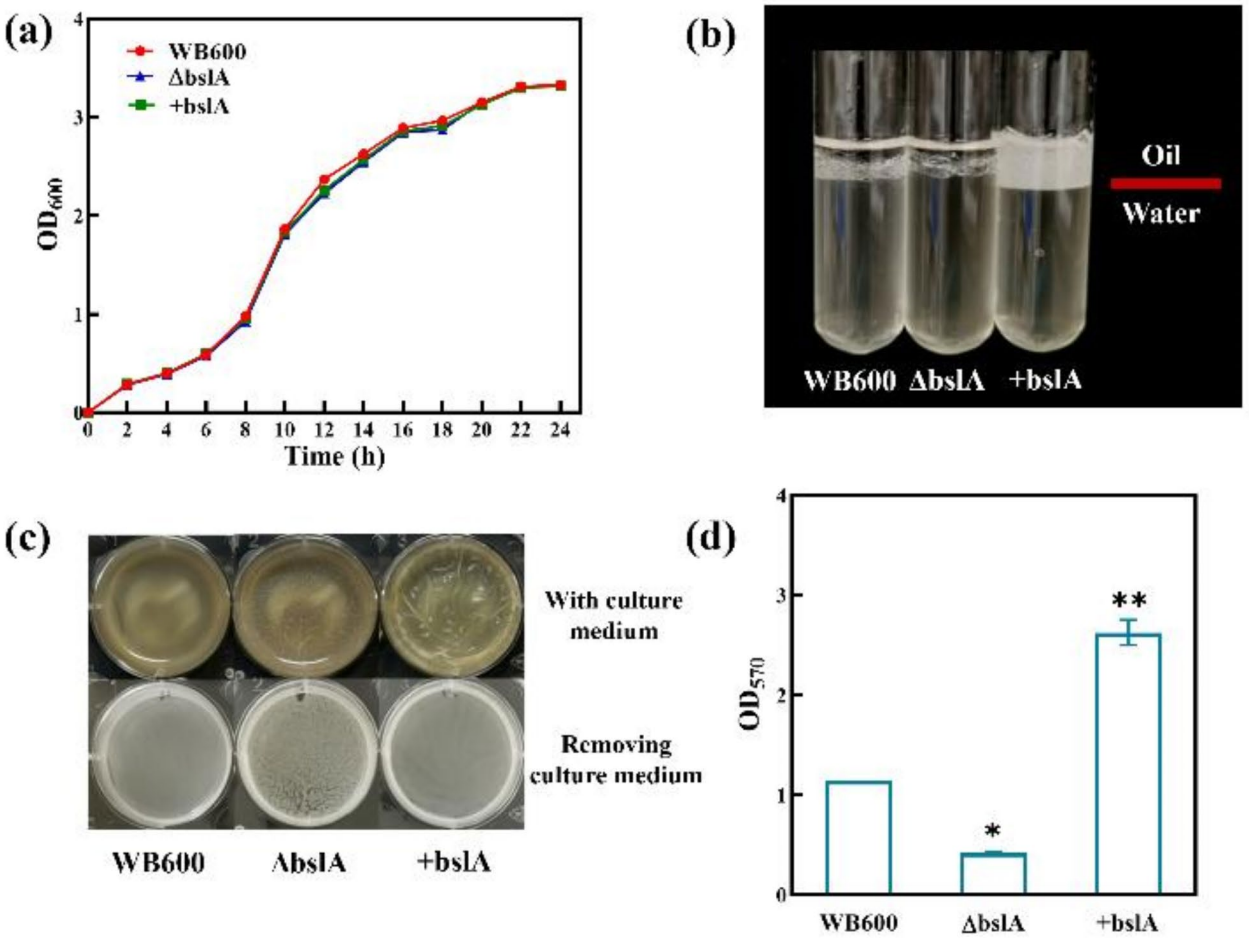

Fig. 2. Effects of hydrophobic protein BslA on biofilms formation. (**a**) Growth curves of strains WB600, ΔbslA and +bslA. (**b**) Comparison of cell surface hydrophobicity of strains WB600, ΔbslA and +bslA. (**c**) Biofilm phenotypes of strains WB600, ΔbslA and +bslA with and without culture medium. (**d**) CV of strains WB600, ΔbslA and +bslA was performed.

	A0	A1	Hydrophobicity (%)
WB600	0.974	0.723	25.77
ΔbslA	0.935	0.734	21.948
+bslA	0.979	0.64	34.627

Table 2. Cell surface hydrophobicity of strains WB600, ΔbslA and + bslA.

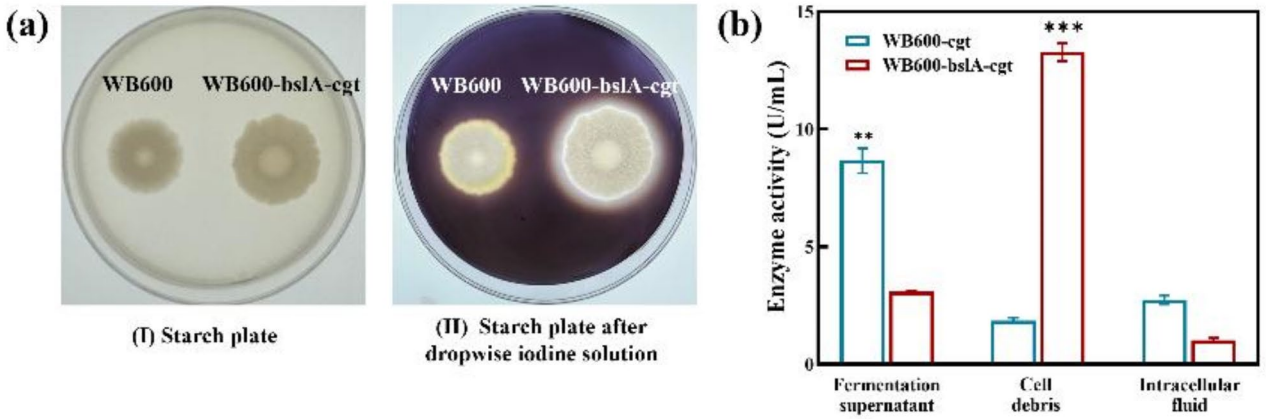

Fig. 3. (**a**) Growth and color development of *B. subtilis* WB600 (**I**) and WB600-bslA-cgt (**II**) in starch plates. (**b**) Assay of enzyme activity of WB600-bslA-cgt and WB600-cgt.

investigated. The changes of cell surface hydrophobicity were calculated in Table 2. Compared to strain WB600, the hydrophobicity of strain ΔbslA decreased by about 4%, while that of strain + bslA increased by about 6%. After vortex mixing and static stratification of the cell suspension, the thinner oil phase of strain ΔbslA was observed compared with strain WB600, while the oil phase of strain + bslA was noticeably thicker (Fig. 2b). During the water-oil separation process, more cells of strain + bslA were transferred from the water phase to the oil phase, indicating that the overexpression of the *bslA* enhanced the hydrophobicity. Both the results and observed phenomena strongly suggested that the overexpression of the *bslA* gene contributed to the improvement of the hydrophobicity.

Furthermore, the study examined the effect of the *bslA* gene on biofilm formation (Fig. 2c). The biofilm formation of strain WB600 appeared uniform and flat. In contrast, strain ΔbslA exhibited a thin and loose biofilm, with numerous visible cracks after removing the medium. Meanwhile, strain + bslA formed folds within the medium, which could stretch again after medium removal. The biofilm formation of strain ΔbslA decreased by 63%. Nevertheless, strain + bslA formed approximately 2.8 times the attached biomass compared to strain WB600 (Fig. 2d). The results indicated that the deficiency of *bslA* led to decreased biofilm formation, while the overexpression of *bslA* favored enhanced biofilm formation.

Expression of surface-displayed β-cyclodextrin glycosyltransferase

The surface-displayed technology could enhance the tolerance and stability of the displayed protein and improve the substrate binding efficiency. In this study, surface-displayed strains were constructed, which the pBE2R plasmid was used as the vector for the display of anchor protein BslA and β-cyclodextrin glycosyltransferase. This strain could catalyze the β-CD production by using the starch as substrate, which resulted in the appearance of the hydrolysis zone after the addition of the iodine solution (Fig. 3a). As the control, strain WB600 was selected and the hydrolysis zone was not observed completely. These results indicated that the strain WB600-bslA-cgt of surface-displayed β-CGTase was successfully constructed with the expression of catalytic activity.

Subsequently, the specific location of the surface-displayed enzyme was determined by measuring β-CGTase enzyme activity in different cellular fractions, including the fermentation supernatant, intracellular fluid, and cell debris. Apparently, the surface-displayed β-CGTase was predominantly located in cell debris, which enzyme activity was 13.27 U/mL (Fig. 3b), owing to the fact that β-CGTase and the anchorin BslA were co-expressed as the fusion protein. These results suggested that strain WB600-bslA-cgt was successfully constructed with enzyme activity. Actually, the carrier protein became part of the biofilms, which was situated in the cell membrane and extended to the outside of the cell wall[25], while the free expression of β-CGTase was mainly concentrated in the fermentation supernatant with enzyme activity of 8.66 U/mL. These results further supported the facts of the successful construction of surface-displayed β-CGTase and accurate positioning of catalytic function.

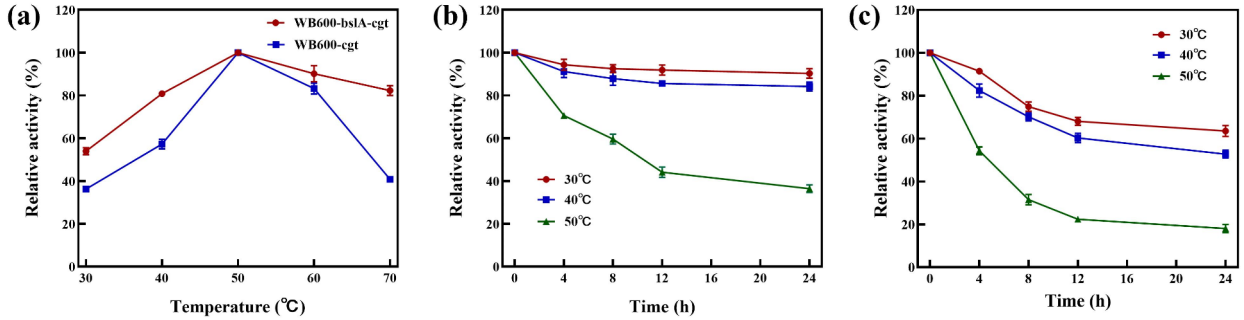

Fig. 4. (**a**) Relative activity of strains WB600-bslA-cgt and WB600-cgt at different reaction temperatures. (**b**) The relative activity of strain WB600-bslA-cgt after being stored at different temperatures for a period of time. (**c**) The relative activity of strain WB600-cgt after being stored at different temperatures for a period of time.

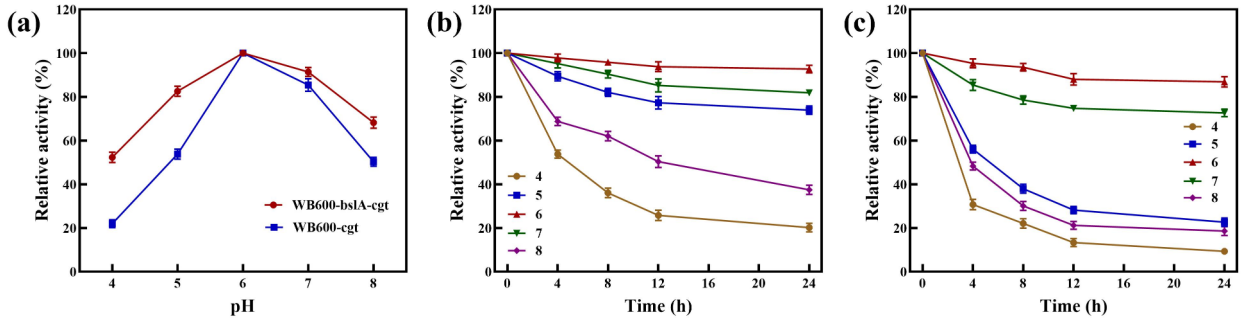

Fig. 5. (**a**) Relative activity of strains WB600-bslA-cgt and WB600-cgt at different reaction pH. (**b**) The relative activity of strain WB600-bslA-cgt after being stored at different pH for a period of time. (**c**) The relative activity of strain WB600-cgt after being stored at different pH for a period of time.

Characterization of surface-displayed β-cyclodextrin glycosyltransferase activity

The influence of temperature and pH on the activity of β-CGTase was detected. The optimal temperature for enzyme activity was consistently 50 °C for both surface-displayed and free cell-expressed β-CGTase, defined as 100% of enzyme activity (Fig. 4a). When relative activity remained above 80%, strain WB600-bslA-cgt exhibited a wider adaptive temperature range compared to strain WB600-cgt (approximately 40 °C Vs 45 °C–60 °C). Figure 4b,c illustrated that the half-life of the surface-displayed enzyme was longer than that of the free-expressed enzyme. After storage for various durations (from 0 h to 24 h) at 30 °C, 40 °C, and 50 °C, the surface-displayed enzyme retained higher activity than the free-expressed enzyme.

For the investigation of pH, variations in enzyme activity and half-life period were observed with similarities to the temperature above. The activity of β-CGTase peaked at pH 6, designated as 100% (Fig. 5a). Relative activity above 80% served as an acceptable standard for the optimal reaction pH. Consequently, the pH range of the surface-displayed enzyme extended from 5.5–7 to 5–7.5, compared to the free-expressed enzyme. Furthermore, the half-life of the surface-displayed enzyme was longer than that of the free-expressed enzyme (Fig. 5b&c). Following treatment at different pH levels (4–8) for varying durations (0–24 h), relative activity remained consistently high.

Studies had reported that a cell surface displayed system in *Pichia pastoris* (*P. pastoris*) GS115 was developed, which showed the *Thermomyces lanuginosus* lipase (*TLL*) with the characteristics of wide thermal adaptability and alkaline pH resistance[37]. Similarly, a displayed cold-adapted chitosanase (CDA) exhibited improved thermostability with the wider temperature and pH ranges compared to the free CDA in *P. pastoris*[38]. These outcomes indicate that a broader and more suitable pH and temperature range for enzymatic reactions could be achieved through surface-displayed enzymes, which exhibited greater stability and extended half-lives.

Free and immobilized cells biocatalytic β-CD production

Free cells biocatalytic β-CD production

The glucose content, the relative activity, and the conversion rate were assessed both in the immobilized catalysis and free cells catalysis using strain WB600-bslA-cgt (Fig. 6a). The whole process could be divided into two phases: cells growth/adsorption and catalysis. In the initial 48 h, strain WB600-bslA-cgt did not show any preference during immobilized catalysis or free cells catalysis in terms of glucose consumption and growth. After the cell growth and adsorption, strain WB600-bslA-cgt entered the catalysis phase, where the highest enzyme activity

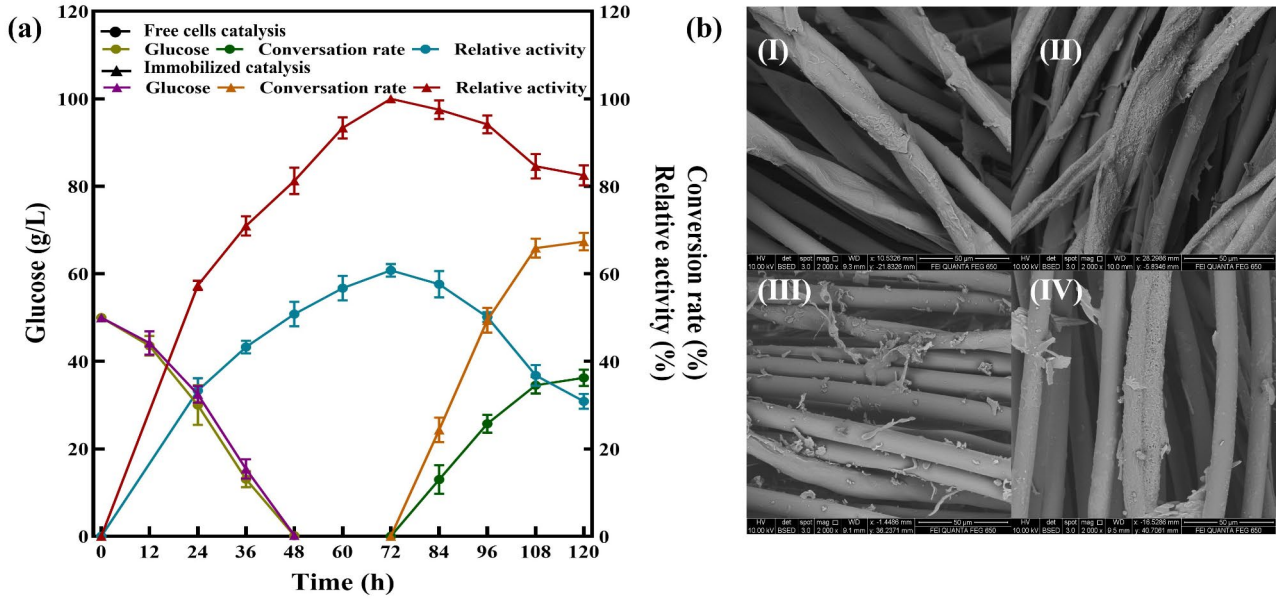

Fig. 6. Single-batch free cells catalysis and biofilm-based immobilized catalysis, and SEM of carriers in single-batch biofilm-based immobilized catalysis. (**a**) Single-batch free cells catalysis and biofilm-based immobilized catalysis of strain WB600-bslA-cgt. (**b**) Scanning electron microscope of carriers in immobilized catalysis of strain WB600-bslA-cgt. (**I**, **II**) Carrier after 24 h and 72 h of fermentation. (**III**) Carrier after 36 h of catalysis. (**IV**) Carrier after 24 h of resuscitation.

was observed at 72 h for both immobilized and free cell catalysis. The enzyme activity of immobilized catalysis at 72 h was defined as 100%. Considering the decrease of relative activity, the production time and cost, the catalytic time was set to 36 h (72–108 h) and the enzymatic reaction solution was replaced when the immobilized continuous catalytic reaction was carried out. After the end of the catalytic reaction, the relative activity of immobilized catalysis was 83%, and the conversion rate was 67%, while the relative activity of free cells catalysis dropped rapidly to 31%, and the conversion rate was only 36%. Benefiting from the protection of biofilms, the cells and enzymes displayed on the surface showed better performance in resisting external stresses in the enzymatic reaction solution, highlighting their potential for sustainable industrial processes[39]. In our previous research, surface-displayed β-galactosidase could continuously catalyze to produce galactooligosaccharide in *P. pastoris*[40]. However, challenges still existed in the system of biofilm-based immobilized fermentation integrating with surface-displayed biocatalysis, including insufficient displayed efficiency, mass transfer and other issues during large-scale fermentation[41,42].

SEM results showed the morphological changes of biofilms during the different phases of fermentation and catalysis (Fig. 6b). In the fermentation phase, cell growth along with adsorption was observed (Fig. 6b I&II). Subsequently, it was used for catalysis process. Due to the difference between the catalytic solution and culture medium, cells were exfoliated from the carriers (Fig. 6b III). Interestingly, after the resuscitation of WB600-bslA-cgt by 24 h, cell growth and adsorption could be recovered as before (Fig. 6b IV), establishing a foundation for continuous catalysis.

Immobilized cells biocatalytic β-CD production

In order to further maximize the advantages of immobilized fermentation integrated with enzyme catalysis, multiple batches continuous catalysis process was investigated. The batch of catalytic reactions was finished when the relative activity was below 60%. In Fig. 7, after 5 times of the continuous catalysis in the Batch 1, the relative activity of enzyme was 57%, which was about 1.8 times that of the single-batch of free cells catalysis. The conversion rate was 40%, which was still 4% higher than the single-batch free cells catalysis (Fig. 6a). For restore the cell vitality, the carriers with cells were taken out then added in the fresh medium for 72 h. After 4 times of the continuous catalysis in the Batch 2, the relative activity was 59% and the conversion rate was 41%. After 4 times of the continuous catalysis in the Batch 3, the relative enzyme activity was 52%, which was about 1.7 times that of the single-batch of free cells catalysis, and the conversion rate was 36%, which was similar with the conversion rate of single-batch free cells catalysis.

Actually, the growth conditions for the strains differed from the reaction conditions for enzyme catalysis. The surface-displayed strains could be degraded partially during the catalytic environment, which resulted in the diminishment of enzyme activity. Hence, after multiple cycles of biocatalysis, the biomass on the carrier was decreased. However, biofilms could shield cells from detrimental external factors[43]. When the relative enzyme activity was reduced to a certain extent, the remained cells in biofilms could quickly resume extensive growth by reintroducing the fresh medium. In general, catalytic time and catalytic efficiency are the important factors in

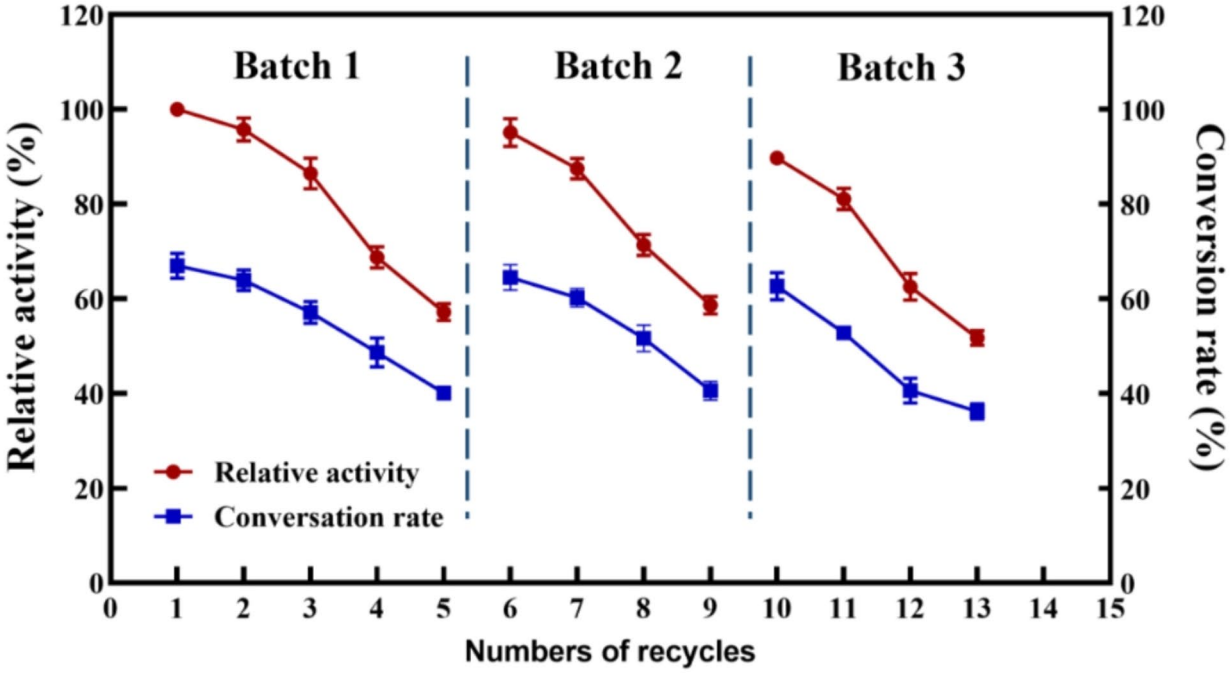

Fig. 7. Number of reuses in the immobilized cell catalysis. When the relative activity dropped to a certain level, the immobilized cells were resuscitated for 72 h before catalysis was resumed.

industrial processes. We used *B. subtilis* combined with biofilm-based continuous biocatalysis to produce β-CD. It reduced the time for subsequent seed culture and cell regrowth/adsorption, and still had high enzyme activity, which was 70% higher than that of the free catalysis compared with the free-cell catalysis of the original strain. These results indicated that it has great potential for efficiently converting valuable products.

Conclusion

In this study, we constructed a biofilm-based immobilized fermentation system, integrating an enzyme catalysis system with surface display in Bacillus subtilis using the hydrophobic protein BslA. The surface-displayed strain exhibited excellent performance in enzyme activity stability, as well as wider temperature and pH tolerance, and a longer half-life. During the continuous catalysis process over 3 batches of 13 times, the relative activity remained around 52%, and the conversion rate exceeded 36%. In conclusion, this study proposed a novel method of catalysis through biofilm-based immobilized fermentation integrated with surface display. This approach provided valuable insights for continuous catalysis and stimulates improvements in industrial biocatalytic processes. Overall, this study represents a successful case of developing biofilm-based continuous catalysis integrated with surface display for the efficient production of β-CD and other biochemicals.

Data availability

Data is provided within the manuscript or supplementary information files.

Received: 7 July 2024; Accepted: 26 November 2024
Published online: 02 December 2024

References

1. Munro, I. C., Newberne, P. M., Young, V. R. & Bar, A. Safety assessment of γ-cyclodextrin. *Regul. Toxicol. Pharmacol.* **39**, 3–13 (2004).
2. Szejtli & József Introduction and general overview of cyclodextrin chemistry. *Chem. Rev.* **98**, 1743–1754 (1998).
3. Gonzalez Pereira, A. et al. Main applications of cyclodextrins in the food industry as the compounds of choice to form host-guest complexes. *Int. J. Mol. Sci.* **22**, 1339 (2021).
4. Mathapa, B. G. & Paunov, V. N. Nanoporous cyclodextrin-based co-polymeric microspheres for encapsulation of active components. *J. Mater. Chem. B.* **1**, 3588–3598 (2013).
5. Morin-Crini, N. & Crini, G. Environmental applications of water-insoluble β-cyclodextrin-epichlorohydrin polymers. *Prog. Polym. Sci.* **38**, 344–368 (2013).
6. Zhu, Q. & Scriba, G. K. E. advances in the use of cyclodextrins as chiral selectors in capillary electrokinetic chromatography: fundamentals and applications. *Chromatographia* **79**, 1403–1435 (2016).
7. Su, L., Li, Y. & Wu, J. Efficient secretory expression of *Bacillus stearothermophilus* α/β-cyclodextrin glycosyltransferase in *Bacillus subtilis*. *J. Biotechnol.* **331**, 74–82 (2021).

8. Urban, M., Beran, M., Adamek, L., Drahoŕd, J. & Matušová, K. Cyclodextrin production from amaranth starch by cyclodextrin glycosyltransferase produced by *Paenibacillus macerans* CCM 2012. *Czech J. Food Sci.* **30**, 15–20 (2012).
9. Man, R. C., Ismail, A. F., Fuzi, S. F. Z. M., Ghazali, N. F. & Illias, R. M. Effects of culture conditions of immobilized recombinant *Escherichia coli* on cyclodextrin glucanotransferase (CGTase) excretion and cell stability. *Process Biochem.* **51**, 474–483 (2016).
10. Gimenez, G. G. et al. Immobilization of commercial cyclomaltodextrin glucanotransferase into controlled pore silica by the anchorage method and covalent bonding. *Process Biochem.* **85**, 68–77 (2019).
11. Rakmai, J. & Cheirsilp, B. Continuous production of β-cyclodextrin by cyclodextrin glycosyltransferase immobilized in mixed gel beads: comparative study in continuous stirred tank reactor and packed bed reactor. *Biochem. Eng. J.* **105**, 107–113 (2016).
12. Chen, T. et al. Biofilm-based biocatalysis for galactooligosaccharides production by the surface display of beta-galactosidase in *Pichia pastoris*. *Int. J. Mol. Sci.* **24**, 6507 (2023).
13. Lozančić, M., Hossain, A. S., Mra, V. & Tepari, R. Surface display-an alternative to classic enzyme immobilization. *Catalysts* **9**, 728 (2019).
14. Gu, Y. et al. Advances and prospects of *Bacillus subtilis* cellular factories: From rational design to industrial applications. *Metab. Eng.* **50**, 109–121 (2018).
15. Oggioni, M. R. et al. Recurrent septicemia in an immunocompromised patient due to probiotic strains of *Bacillus subtilis*. *J. Clin. Microbiol.* **36**, 325–326 (1998).
16. Cheng, J., Zhuang, W., Li, N., Tang, C. & Ying, H. Efficient biosynthesis of D-ribose using a novel co-feeding strategy in *Bacillus subtilis* without acid formation. *Lett. Appl. Microbiol.* **64**, 73–78 (2017).
17. Westbrook, A. W., Xiang, R., Murray, M. Y. & Perry, C. C. Engineering of cell membrane to enhance heterologous production of hyaluronic acid in *Bacillus subtilis*. *Biotechnol. Bioeng.* **115** (2018).
18. Kim, D., Kim, W. & Kim, J. New bacterial surface display system development and application based on *Bacillus subtilis* YuaB Biofilm component as an anchoring motif. *Biotechnol. Bioprocess. Eng.* **26**, 39–46 (2021).
19. Gupta, R. & Noronha, S. B. Utilization of *Bacillus subtilis* cells displaying a glucose-tolerant beta-glucosidase for whole-cell biocatalysis. *Enzym. Microb. Technol.* **132**, 109444 (2020).
20. Blankenship, J. R. & Mitchell, A. P. How to build a biofilm: A fungal perspective. *Curr. Opin. Microbiol.* **9**, 588–594 (2006).
21. Li, Z. et al. Involvement of glycolysis/gluconeogenesis and signaling regulatory pathways in *Saccharomyces cerevisiae* biofilms during fermentation. *Front. Microbiol.* **6**, 139, (2015).
22. Liang, C., Ding, S., Sun, W., Liu, L. & Chen, Y. Biofilm-based fermentation: A novel immobilisation strategy for *Saccharomyces cerevisiae* cell cycle progression during ethanol production. *Appl. Microbiol. Biotechnol.* **104**, 7495–7505 (2020).
23. Liu, Q., Zhao, N., Zou, Y., Ying, H. & Chen, Y. Feasibility of ethanol production from expired rice by surface immobilization technology in a new type of packed bed pilot reactor. *Renew. Energy*. **149**, 321–328 (2020).
24. Morris, R. J., Bromley, K. M., Stanley-Wall, N. & MacPhee, C. A phenomenological description of BslA assemblies across multiple length scales. *Philos. Trans. R. Soc. A Math. Phys. Eng. Sci.* **374**, 20150131 (2016).
25. Arnaouteli, S., MacPhee, C. E. & Stanley-Wall, N. R. Just in case it rains: Building a hydrophobic biofilm the *Bacillus subtilis* way. *Curr. Opin. Microbiol.* **34**, 7–12 (2016).
26. Epstein, A. K., Pokroy, B., Seminara, A. & Aizenberg, J. Bacterial biofilm shows persistent resistance to liquid wetting and gas penetration. *Proc. Natl. Acad. Sci.* **108**, 995–1000 (2011).
27. Penninga, D. et al. The raw starch binding domain of cyclodextrin glycosyltransferase from *Bacillus circulans* strain 251. *J. Biol. Chem.* **271**, 32777–32784 (1996).
28. Wang, H., Wang, Y. & Yang, R. Recent progress in *Bacillus subtilis* spore-surface display: Concept, progress, and future. *Appl. Microbiol. Biotechnol.* **101**, 933–949 (2017).
29. Mel, R. Microbial adhesion to hydrocarbons: Twenty-five years of doing MATH. *FEMS Microbiol. Lett.* **262**, 129–134 (2006).
30. Bonnekoh, B., Wevers, A., Jugert, F., Merk, H. & Mahrle, G. Colorimetric growth assay for epidermal cell cultures by their crystal violet binding capacity. *Arch. Dermatol. Res.* **281**, 487–490 (1989).
31. Magana, M. et al. Options and limitations in clinical investigation of bacterial biofilms. *Clin. Microbiol. Rev.* **31**, e00084–e00016 (2018).
32. Sun, W. et al. Blue light signaling regulates *Escherichia coli* W1688 biofilm formation and L-threonine production. *Microbiol. Spectr.* **10**, e02460–e02422 (2022).
33. Thibeaux, R., Kainiu, M. & Goarant, C. Biofilm formation and quantification using the 96-microtiter plate. *Methods Mol. Biol.* **2134**, 207–214 (2020).
34. Han, R. et al. Carbohydrate-binding module-cyclodextrin glycosyltransferase fusion enables efficient synthesis of 2-O-d-glucopyranosyl-l-ascorbic acid with soluble starch as the glycosyl donor. *Appl. Environ. Microbiol.* **79**, 3234–3240 (2013).
35. Penninga, D. et al. Site-directed mutations in tyrosine 195 of cyclodextrin glycosyltransferase from *Bacillus circulans* strain 251 affect activity and product specificity. *Biochemistry* **34**, 3368–3376 (1995).
36. Mäkelä, M., Korpela, T. & Laakso, S. Colorimetric determination of β-cyclodextrin: Two assay modifications based on molecular complexation of phenolphatalein. *J. Biochem. Biophys. Methods*. **14**, 85–92 (1987).
37. Yang, J. et al. Cell surface display of *Thermomyces lanuginosus* lipase in *Pichia pastoris*. *Front. Bioeng. Biotechnol.* **8**, 544058 (2020).
38. Peng, Y. et al. Expression and surface display of an acidic cold-active chitosanase in *Pichia pastoris* using multi-copy expression and high-density cultivation. *Molecules* **27**, 800 (2022).
39. Rumbaugh, K. P. & Sauer, K. Biofilm dispersion. *Nat. Rev. Microbiol.* **18**, 571–586 (2020).
40. Chen, T. et al. Biofilm-based biocatalysis for galactooligosaccharides production by the surface display of β-Galactosidase in *Pichia pastoris*. *Int. J. Mol. Sci.* **24**, 6507 (2023).
41. Hewitt, C. J. & Nienow, A. W. The scale-up of microbial batch and fed-batch fermentation processes. *Adv. Appl. Microbiol.* **62**, 105–135 (2007).
42. Schüürmann, J., Quehl, P., Festel, G. & Jose, J. Bacterial whole-cell biocatalysts by surface display of enzymes: Toward industrial application. *Appl. Microbiol. Biotechnol.* **98**, 8031–8046 (2014).
43. Flemming, H-C. & Wingender, J. The biofilm matrix. *Nat. Rev. Microbiol.* **8**, 623–633 (2010).

Author contributions

Dan Wang: Conceptualization, Supervision, Validation, Writing-review & editing. Sinan Wang: Investigation Data curation, Visualization. Wenjun Sun: Conceptualization, Supervision, Writing-Review editing. Tianpeng Chen: Conceptualization, Supervision, Writing-Review editing. Caice Liang: Methodology, Data curation, Visualization, Writing–original draft. Pengpeng Yang: Conceptualization, Funding Acquisition. Qingguo Liu: Funding Acquisition. Chunguang Zhao: Funding Acquisition. Yong Chen: Conceptualization, Funding Acquisition. All authors have given approval to the final version of the manuscript.

Funding

This work was supported by the National Key R&D Program of China (2022YFC2105400); the National Natural Science Foundation of China (22178176; 22208157); Jiangsu National Synergetic Innovation Center for

Advanced Materials (SICAM-XTA2201); the Youth Fund of Natural Science Foundation of Jiangsu Province (BK20220334); the Key R&D project of Ningxia Hui Autonomous Region (2023BEE01011). the State Key Laboratory of Materials-Oriented Chemical Engineering (SKL-MCE-22A04).

Declarations

Competing interests

The authors declare no competing interests.

Additional information

Supplementary Information The online version contains supplementary material available at https://doi.org/10.1038/s41598-024-81490-z.

Correspondence and requests for materials should be addressed to W.S. or T.C.

Reprints and permissions information is available at www.nature.com/reprints.

Publisher's note Springer Nature remains neutral with regard to jurisdictional claims in published maps and institutional affiliations.